

Supplemental Information

MALT1 Small Molecule Inhibitors Specifically

Suppress ABC-DLBCL In Vitro and In Vivo

Lorena Fontan, Chenghua Yang, Venkataraman Kabaleeswaran, Laurent Volpon, Michael J. Osborne, Elena Beltran, Monica Garcia, Leandro Cerchietti, Rita Shaknovich, Shao Ning Yang, Fang Fang, Randy D. Gascoyne, Jose Angel Martinez-Climent, J. Fraser Glickman, Katherine Borden, Hao Wu, and Ari Melnick

Inventory of Supplemental Information

Supplemental Data

Figure S1. Related to Figure 1

Figure S2. Related to Figure 2

Figure S3. Related to Figure 3

Figure S4. Related to Figure 4

Table S1. Related to Figure 5

Figure S5. Related to Figure 5

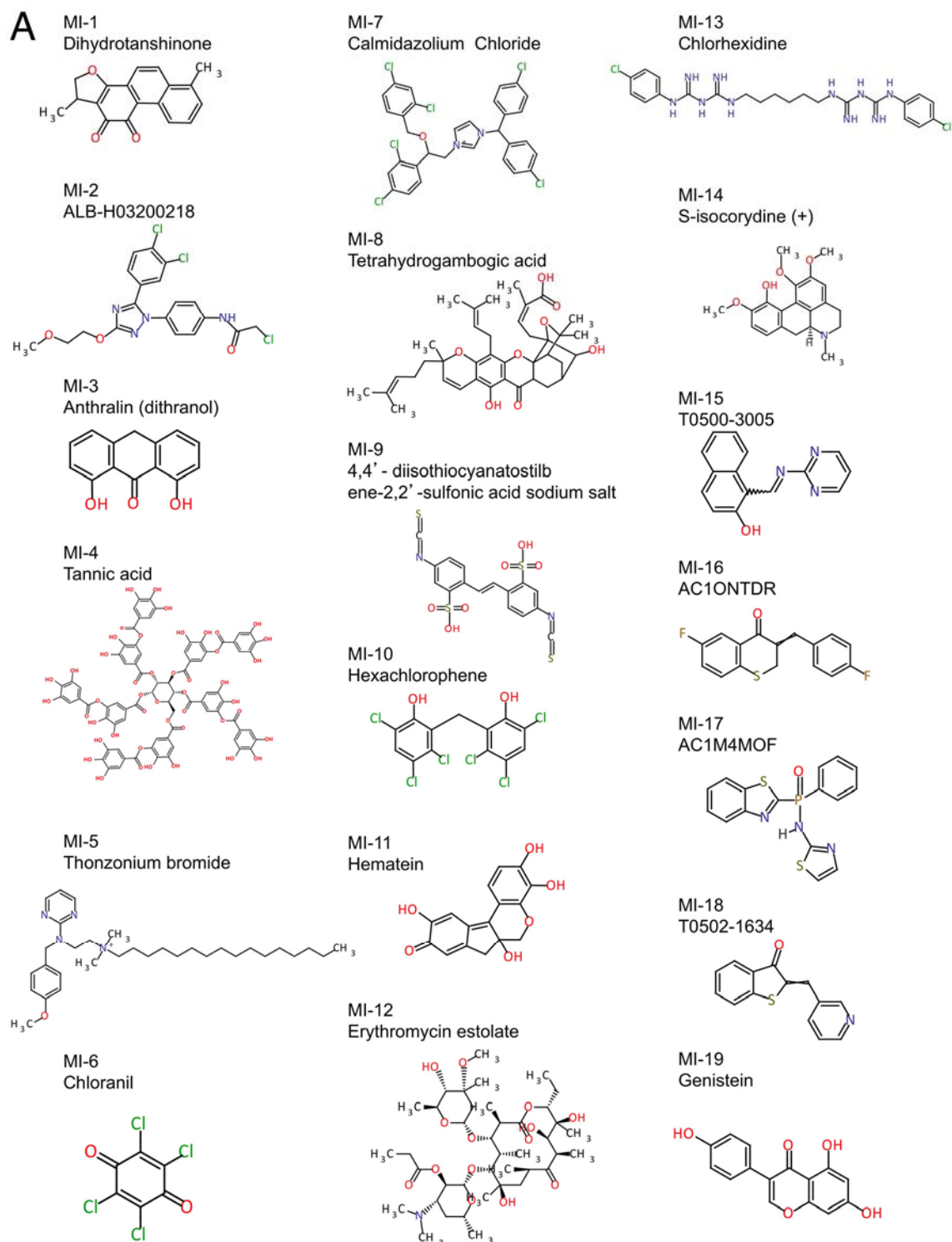
Table S2. Related to Figure 6

Figure S6. Related to Figure 7

Supplemental Experimental Procedures

Supplemental References

Supplemental Data



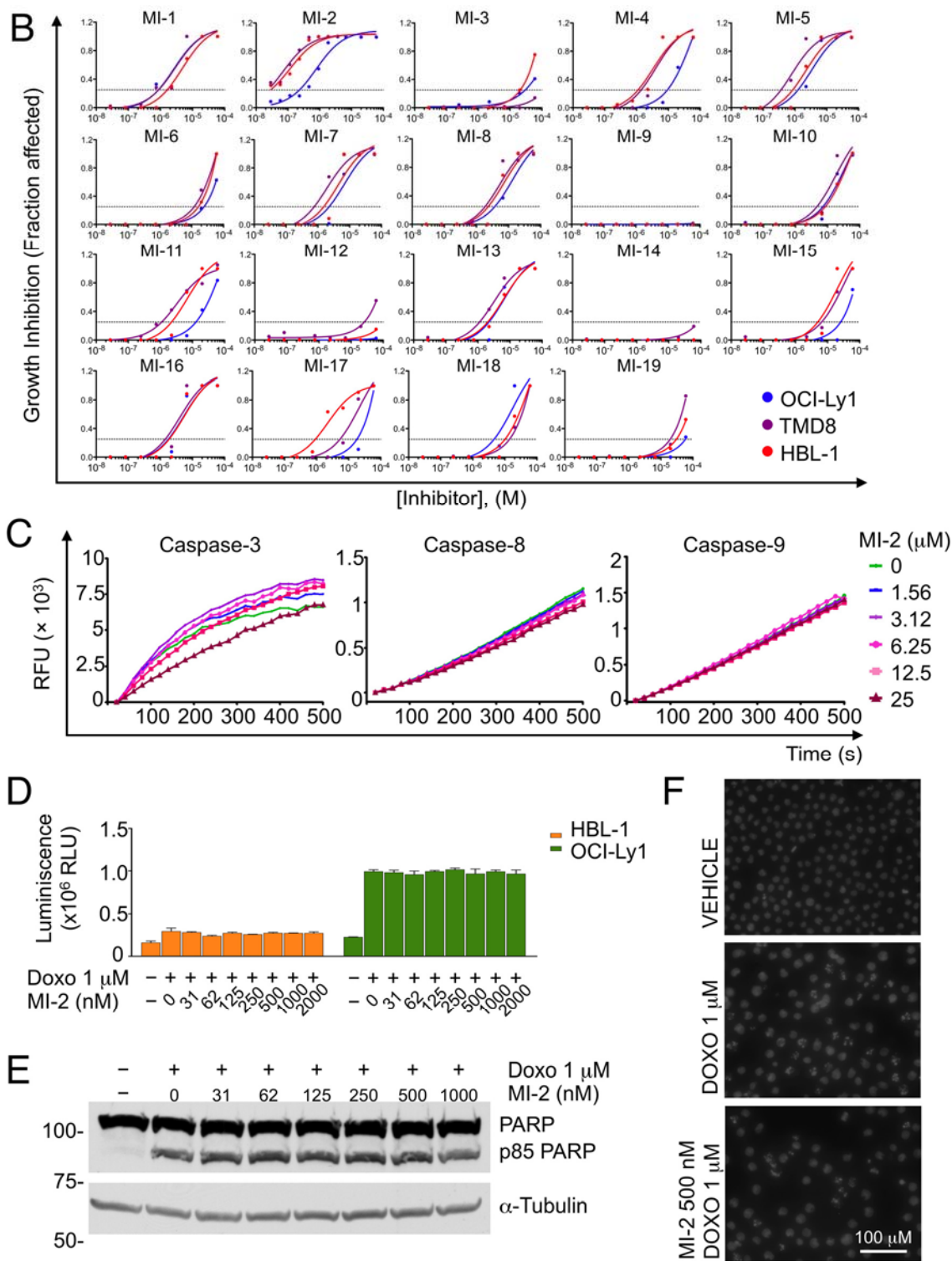


Figure S1, related to Figure 1. Identification of MALT1 inhibitors and lack of effect on related caspases. (A) Hit compounds validated in biochemical and cell-based assays. (B) Growth inhibition (GI) curves for all 19 compounds assayed in HBL-1, TMD8 and OCI-OCI-Ly1 cells. The y-axis

represents GI (fraction affected relative to vehicle). The x-axis represents dose of the inhibitor tested. Results are mean of three independent experiments performed in triplicate. Dotted line cuts at $y = GI_{25}$. GI_{25} values are summarized in Figure 1B. (C) Cleavage of the Ac-DEVD-AFC substrate (50 μ M) by Caspase-3 (100 nM), the Ac-DEVD-AMC substrate (10 μ M) by Caspase-8 (20 nM) and the Ac-LEHD-AFC substrate (100 μ M) by Caspase-9 (200 nM) is plotted as a function of time in Relative Fluorescence Units (RFU $\times 10^3$). Effects of MI-2 at up to 25 μ M, the solubility limit of the compound, are shown. There is virtually no effect for Caspase-8 and -9. There is also very little effect on Caspase-3, and the data cannot be fit to obtain the IC_{50} value, which is $\gg 25 \mu$ M. (D) HBL-1 and OCI-Ly1 cells were exposed to 1 μ M doxorubicin for 48 hours, then treated with increasing concentration of MI-2 for 2 hours and assayed for Caspase-3/-7 activity using the CaspaseGLO reagent DEVD-aminoluciferin that emits luminescence upon cleavage. The y-axis represents luminescence ($\times 10^6$ Relative Light Units). Results are mean \pm SD of one representative experiment performed in triplicate. The experiment was performed three times with similar results. (E) Western blot of PARP in MALT1 independent OCI-Ly1 cells following treatment for 48 hr with doxorubicin was used to assess MI-2 effect on PARP cleavage. Cells were pretreated for 30 minutes with indicated concentrations of MI-2. α -Tubulin is shown as a loading control. (F) Cells were pretreated for 30 minutes with 500 nM of MI-2 followed by treatment for 48 hr with doxorubicin. And impact of MI-2 on doxorubicin induced nuclear fragmentation in MALT1 independent OCI-Ly1 cells was evaluated by Hoechst 33342 staining. Fragmented nuclei number relative to total nuclei was evaluated.

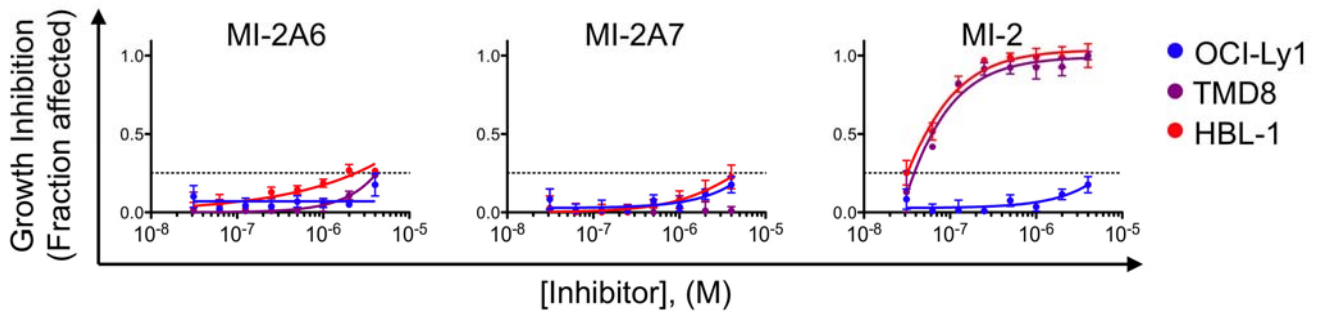
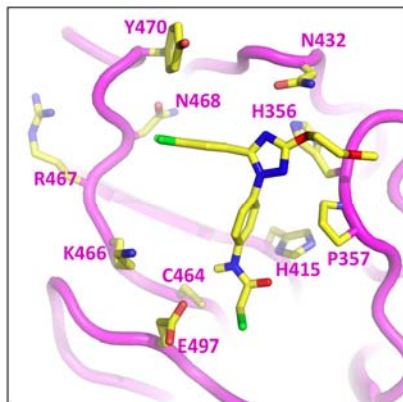


Figure S2, related to Figure 2. Effect of negative control compounds on cell growth. Growth inhibition curves of the inactive analogs: MI-2A6 and MI-2A7 in HBL-1, TMD8 and OCI-Ly1 cells. Results for MI-2 are shown for comparison. The y-axis represents Growth Inhibition (fraction affected relative to vehicle). The x-axis represents dose of the inhibitor tested. Results are represented as mean \pm SEM. The assay was performed three times in triplicate.

A



B

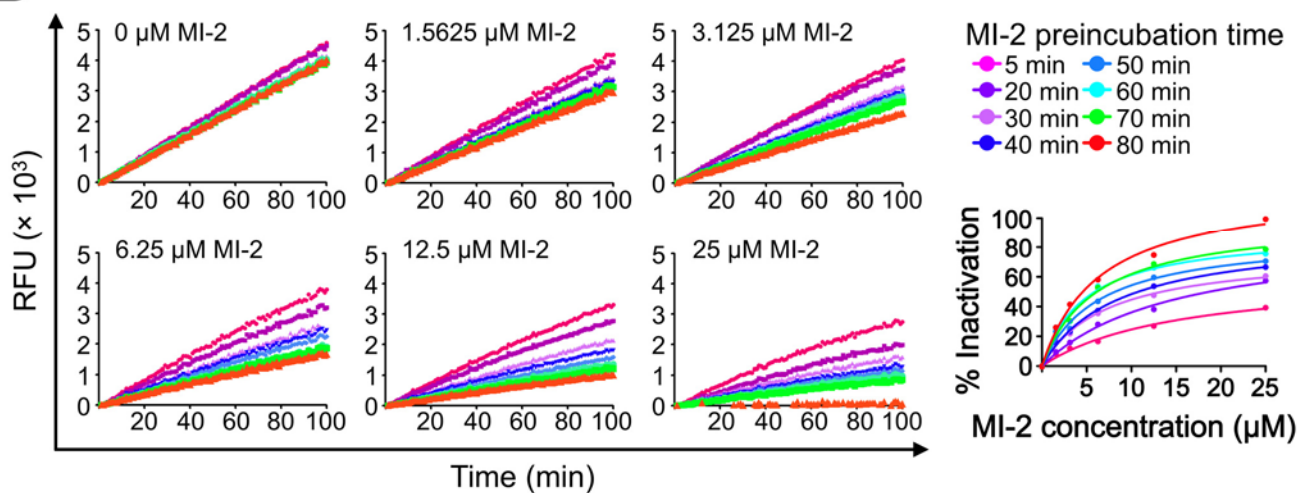


Figure S3, related to Figure 3. Analog compounds to MI-2 display similar effects to MI-2. (A) Detailed environment of docked MI-2 (in stick model) on MALT1 (in ribbon model with residues detail in stick model). Residues surrounding MI-2 are labeled. (B) Progress curves of MALT1-cleavage activity with different pre-incubation time (5 minutes to 80 minutes) and at different MI-2 concentrations (0-25 μM). The panel in the box represents the summarized normalized percentage of MALT1 inactivation as a function of MI-2 concentration at different pre-incubation times showing both preincubation time- and concentration-dependent inactivation of MALT1 by MI-2.

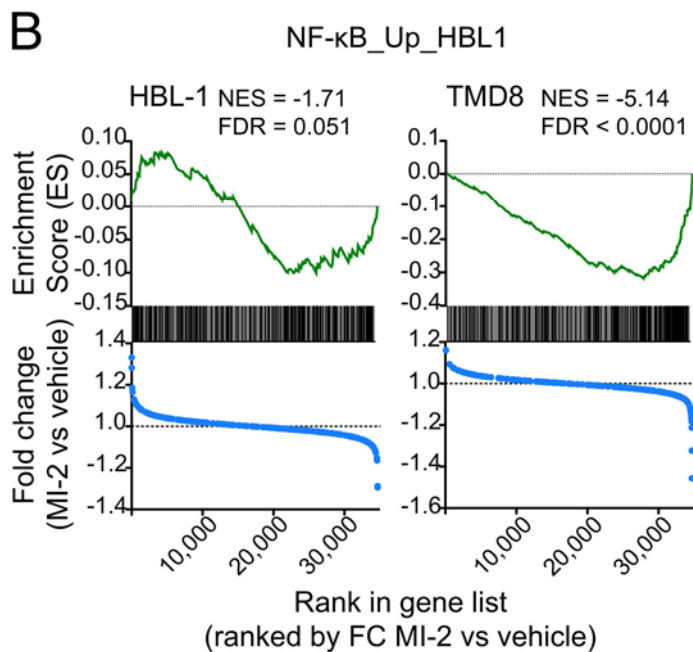
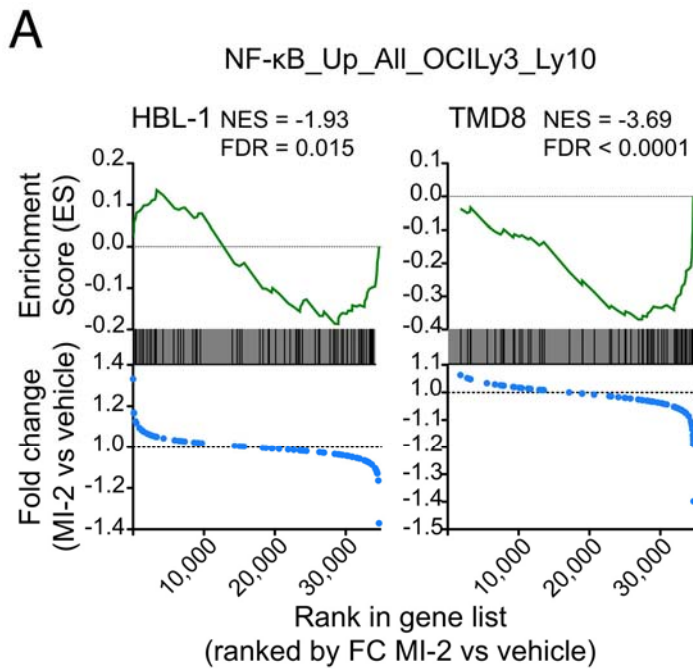


Figure S4, related to Figure 4. MI-2 effects on cell signaling. (A) GSEA plots representing the enrichment of NF- κ B induced target genes (NF- κ B target gene signature NF- κ B_Up_All_OCILy3_Ly10) (Lam et al., 2005) among genes downregulated after MI-2-treatment in HBL-1 and TMD8 cells. Normalized Enrichment Score (NES) and FDR values are indicated. The top plot represents enrichment score compared to position of signature genes in the ranked dataset (green

tracing). The bottom plot represents fold change gene expression in MI-2 vs. vehicle compared to position of signature genes in the ranked dataset (blue tracing). (B) GSEA performed using the NF- κ B signature NF- κ B_Up_HBL1 (available online at http://lymphochip.nih.gov/cgi-bin/signaturedb/signatureDB_DisplayGenes.cgi?signatureID=276), represented as described in (A).

Table S1, related to Figure 5. ABC-DLBCL NF- κ B activating mutations present in the cell lines used in this study.

| Cell line | CD79A/B (Davis et al., 2010) | MYD88 (Ngo et al., 2011) | CARD11 (Lenz et al., 2008) | TNFAIP3 (Compagno et al., 2009) | TAK1 (Compagno et al., 2009) |
|------------------|---|---|---|--|---|
| HBL-1 | Y196F ^{HET} | L265P | WT | WT | WT |
| TMD8 | Y196H ^{HET} | L265P | WT | WT | WT |
| OCI-Ly3 | WT | L265P | L251P | Hem del | WT |
| OCI-Ly10 | Δ 4275-4316 ^{HET} | L265P | WT | Hem del | WT |
| U2932 | WT | WT | WT | Hem del | S417A |
| HLY-1 | WT | S219C | E634Q | Hom del | WT |
| OCI-Ly7 | WT | WT | WT | WT | WT |
| OCI-Ly1 | WT | WT | WT | WT | WT |

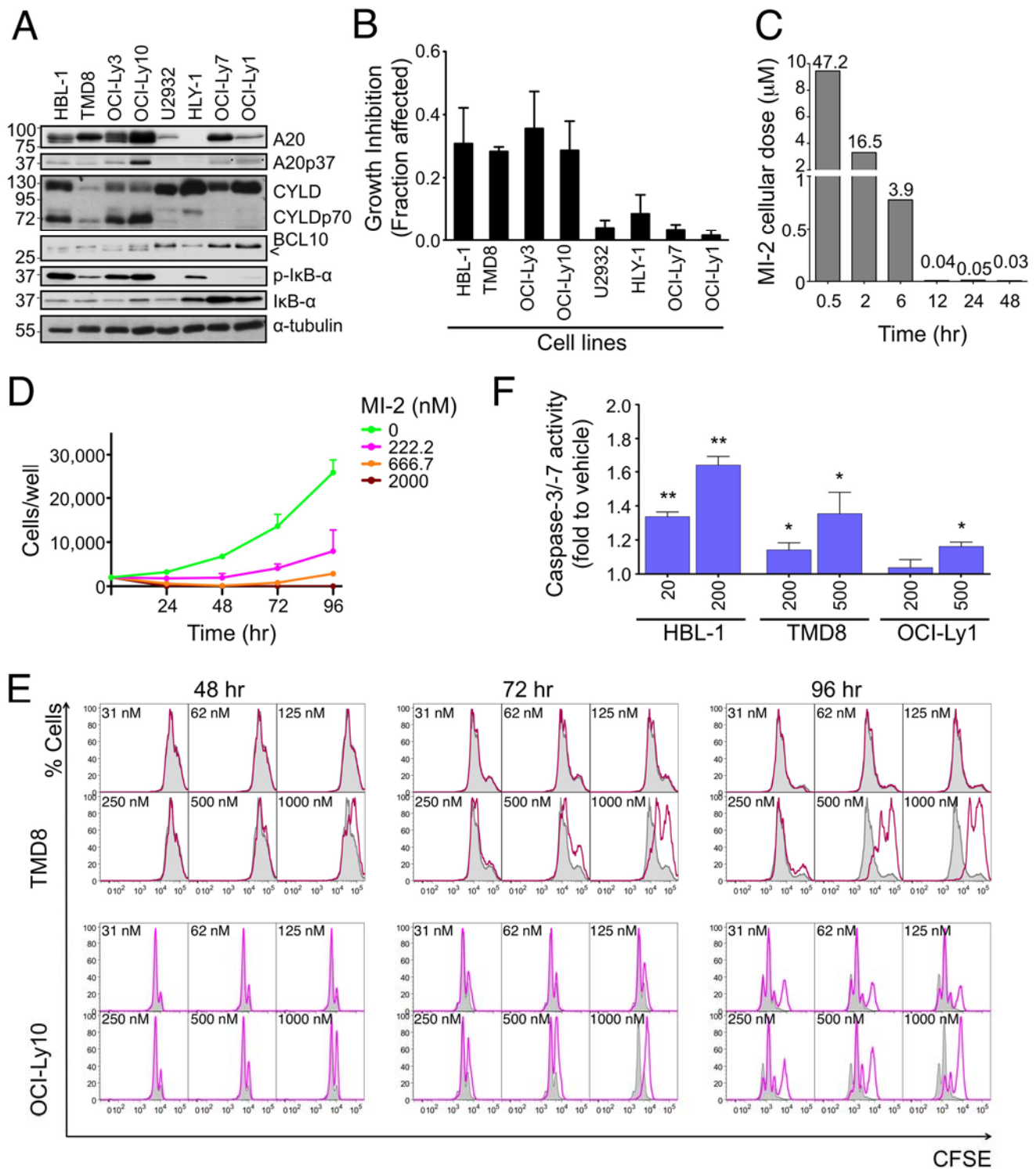


Figure S5, related to Figure 5. Biologic effects of MI-2 on DLBCL cells. (A) MALT1 activation status determined in a panel of DLBCL cell lines by Western blotting of its cleavage target proteins A20, CYLD and Bcl10. NF- κ B activation was confirmed by IkB and phospho-IkB expression. <

Cleavage product. * Unspecific band. (B) Cell growth dependence on MALT1 cleavage activity in indicated cell lines was assessed using the Z-VRPR-FMK peptide inhibitor at 50 μ M for 48 hour. The y-axis represents Growth Inhibition (mean \pm SD) relative to vehicle-treated cells. (C) Time-dependent intracellular concentration of MI-2 was determined using liquid chromatography-mass spectroscopy (LC-MS) in HBL-1 cells treated with 0.2 μ M MI-2. Samples were collected at 30 min, 2, 6, 12, 24 and 48 hours. The y-axis represents detected MI-2 intracellular concentration. The x-axis represents exposure time. (D) HBL-1 cells were treated once at t-0 with increasing concentrations of MI-2 and cell viability was evaluated every 24 hr for 4 days using an ATP-metabolic assay. A standard curve was used to interpolate cell number. The y-axis represents cell number/well; the x-axis, time of treatment. Results are mean \pm SEM of three independent experiments done in triplicate. (E) Flow cytometric determination of CFSE fluorescence of 2×10^4 TMD8 and OCI-Ly10 cells after treatment with increasing doses of MI-2 as indicated 48, 72 and 96 hours after treatment. The y-axis represents % cells. The x-axis represents CFSE labeling. DAPI^{neg} cells were gated for analysis. (F) DLBCL cell lines as indicated were exposed to GI₂₅ and GI₅₀ concentrations of MI-2 for 48 hours assayed for Caspase-3/-7 activity using the CaspaseGLO reagent DEVD-aminoluciferin that emits luminescence upon cleavage. The y-axis represents luminescence fold change relative to vehicle treated cells. Data are mean \pm SD of two independent experiments performed in triplicate. Statistics: t- test; * $p < 0.05$, ** $p < 0.01$. Caspase cleavage was significantly increased in the two ABC-DLBCL cell lines at both GI₂₅ and GI₅₀ concentrations. At the higher dose level there was a small but significant amount of Caspase cleavage detected in OCI-Ly1 cells. This effect in OCI-Ly1 cells reflects the sensitivity of the CaspaseGlo assay to detect small levels of cleavage. While ABC-DLBCL are more addicted to and display higher basal activation of MALT1 signaling and its upstream triggers, these pathways are still functional in GCB-DLBCL cells and likely explain this result in OCI-Ly1 cells, which are nonetheless clearly biologically resistant to MALT1 inhibition as shown in Figure 5 and subsequent Figures in vivo.

Table S2, related to Figure 6. Cell blood count and serum chemistry results from the Toxicity 2 experiment (25 mg/kg IP daily administration of MI-2 or equivalent volume of vehicle for 14 days).

| Test | Vehicle | MI-2_day 14 | MI-2_day 24 | Reference | Units |
|----------------------|---------|-------------|-------------|-----------|------------|
| ALP | 92.6 | 83 | 100 | 23-181 | U/L |
| ALT | 29.6 | 25 | 23 | 16-58 | U/L |
| AST | 98.4 | 70 | 49.5 | 36-102 | U/L |
| CK | 885.8 | 202.8 | 119.5 | 358-1119 | U/L |
| GGT | 0 | 0 | 0 | | U/L |
| ALBUMIN | 3.26 | 3.12 | 3.15 | 2.5-3.9 | g/dL |
| TOTAL PROTEIN | 5.64 | 5.32 | 5.30 | 4.1-6.4 | g/dL |
| GLOBULIN | 2.38 | 2.20 | 2.15 | 1.3-2.8 | g/dL |
| TOTAL BILIRUBIN | 0.220 | 0.180 | 0.175 | 0-0.3 | mg/dL |
| DIRECT BILIRUBIN | 0.04 | 0.10 | 0.10 | | mg/dL |
| INDIRECT BILIRUBIN | 0.18 | 0.08 | 0.07 | | mg/dL |
| BUN | 26.6 | 23.4 | 27.0 | 14-32 | mg/dL |
| CREATININE | 0.24 | 0.22 | 0.20 | 0.1-0.6 | mg/dL |
| CHOLESTEROL | 87.8 | 85.4 | 91.75 | 70-100 | mg/dL |
| GLUCOSE ^a | 320.6 | 313.8 | 288.5 | 76-222 | mg/dL |
| CALCIUM | 11.06 | 10.88 | 10.80 | 7.6-10.7 | mg/dL |
| PHOSPHORUS | 10.62 | 9.46 | 9.65 | 4.6-10.5 | mg/dL |
| CHLORIDE | 107.4 | 108.4 | 106.7 | 103-115 | mEq/L |
| SODIUM | 154.2 | 152.8 | 153 | 148-154 | mEq/L |
| WBC | 7.98 | 7.83 | 9.03 | 5.4-16 | K/ μ L |
| RBC | 7.44 | 8.60 | 9.38 | 6.7-9.7 | M/ μ L |
| HEMOGLOBIN | 12.15 | 12.94 | 13.55 | 10.2-10.6 | g/dL |
| HEMATOCRIT | 35.77 | 40.86 | 45.02 | 32-54 | (%) |
| NEUTROPHILS | 1.19 | 1.18 | 1.85 | 0-1.8 | K/ μ L |
| LYMPHOCYTES | 6.26 | 6.29 | 6.76 | 2.5-10 | K/ μ L |
| MONOCYTES | 0.27 | 0.32 | 0.27 | 0-0.2 | K/ μ L |
| EOSINOPHILS | 0.21 | 0.03 | 0.11 | 0-0.5 | K/ μ L |
| BASOPHILS | 0.04 | 0.01 | 0.04 | 0-0.4 | K/ μ L |
| PLATELETS | 468 | 981 | 1275 | 799-1300 | K/ μ L |

^a There was a mild increase in glucose in both vehicle and MI-2 treated animals perhaps due to administration of dextrose as an excipient, or because mice were not fasting.

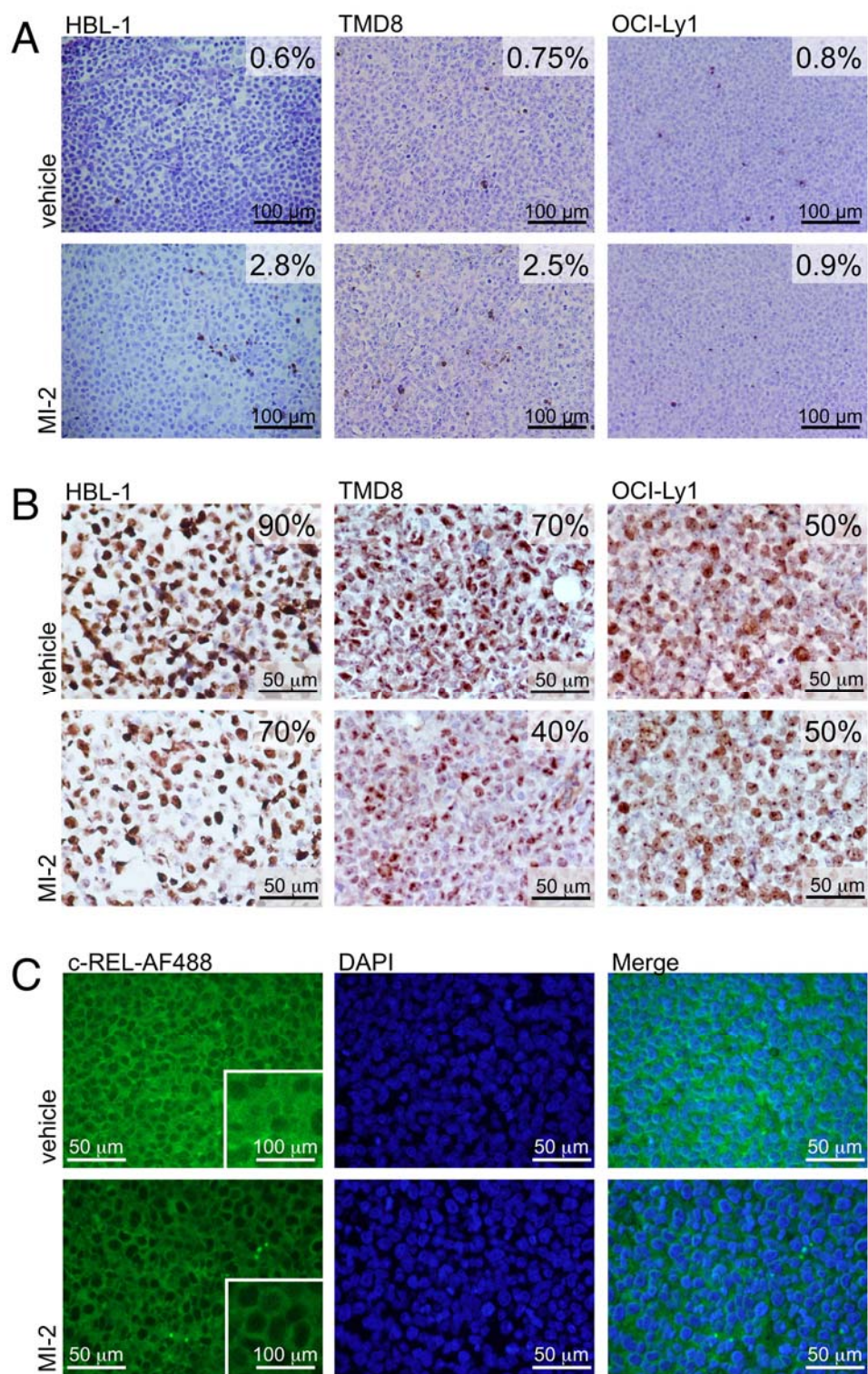


Figure S6, related to Figure 7. Immunohistochemistry in xenografted tumors. Representative micrographs of TUNEL assay (A) and Ki-67 staining (B) for HBL-1, TMD8 and OCI-Ly1 xenografted tumors treated for 14 consecutive days with 25 mg/kg of MI-2 or the same amount of vehicle. (C) c-

REL immunohistochemical staining in sections from TMD8 xenografts exposed to MI-2 (25 mg/kg) or vehicle. Insets are 2 × digital amplification. Representative image of 3 HPF analyzed for n=5 tumors stained for each treatment.

Supplemental Experimental Procedures

High-Throughput Screening for MALT1 Proteolytic Activity Inhibitors

The screening consisted of a 20 μ l reaction in 384-well black plates (Greiner Bio One, Wemmel, Belgium, catalogue # 784076) with 100 nM LZ-MALT1, 200 μ M Ac-LRSR-AMC, and 12.5 μ M test compound in buffer A (20 mM HEPES pH 7.5, 10 mM KCl, 1.5 mM MgCl₂, 1 mM EDTA, 1 mM DTT, 0.01% Triton X-100). The reactions were measured with excitation/emission wavelengths of 360/465 nm using Envision Multilabel Reader (Perkin-Elmer, Waltham, MA). Two time points were measured for each reaction; the fluorescence difference between time points (T2-T1) was considered as MALT1 activity to eliminate false positives due to compound autofluorescence. Average of control values was used in the calculation of percent inhibition. The final percent inhibition was calculated with the formula: $\{[\text{fluorescence}_{\text{test compound}(T2-T1)} - \text{fluorescence}_{\text{neg ctrl}(T2-T1)}] / [\text{fluorescence}_{\text{pos ctrl}(T2-T1)} - \text{fluorescence}_{\text{neg ctrl}(T2-T1)}]\} \times 100$. Z-VRPR-FMK (300 nM) was used as positive control; buffer only was used as negative control. Using 40% inhibition as a threshold, 324 compounds were identified as potential MALT1 inhibitors. The positive hits were validated in concentration-response experiments within a dose range of 0.122 μ M to 62.5 μ M to determine IC₅₀ (50% of inhibition) of the compounds. Activity was also validated using recombinant full-length wild-type MALT1 in addition to the LZ-MALT1 used for screening.

Protein Expression and Purification

MALT1 (340-789) was fused with leucine-zipper sequence from GCN4 (251–281) in the N-terminus (LZ-MALT1). N-terminal his-tagged LZ-MALT1 was expressed in E. Coli and purified by Ni-NTA affinity chromatography (Qiagen, Valencia, CA) followed by gel filtration chromatography with Superdex 200 HR 10/300 (GE Healthcare, UK) in buffer containing 20 mM Tris (pH 7.5), 150 mM NaCl, and 5 mM DTT.

Cell Culture

DLBCL cell lines OCI-Ly1, OCI-Ly7 and OCI-Ly10 were grown in 80% Iscove's medium, 20% FBS and penicillin G/streptomycin. DLBCL cell lines HBL-1, TMD8, U2932 were cultured in 90% RPMI medium, 10% FBS, 2 mM glutamine, 10 mM Hepes and penicillin G/streptomycin. DLBCL cell lines OCI-Ly3 and HLY1 were cultured in 80% RPMI medium, 20% FBS, 2 mM glutamine, 10 mM Hepes and penicillin G/streptomycin. 293T cells were cultured in 90% D-MEM, 10% FBS and penicillin G/streptomycin. All cell lines were cultured at 37°C in a humidified atmosphere of 5% CO₂. Cell lines were authenticated by single nucleotide polymorphism profiling (fingerprinting).

Growth-Inhibition Determination

DLBCL cell lines were grown in exponential growth conditions during the 48 hr of treatment. Cell proliferation was determined by ATP quantification using a luminescent method (CellTiter-Glo, Promega, Madison, WI) and Trypan blue dye-exclusion (Sigma, St. Louis, MO). Luminescence was measured using the Synergy4 microplate reader (BioTek Instruments, Winooski, VT). Standard curves for each cell line were calculated by plotting the cell number (determined by the Trypan blue method) against their luminescence values and number of cells was calculated accordingly. Cell viability in drug-treated cells was normalized to their respective controls (fractional viability) and results are given as 1-fractional viability. CompuSyn software (Biosoft, Cambridge, UK) was used to determine the drug concentration that inhibits the growth of cell lines by 25% compared to control (GI₂₅). Experiments were performed in triplicate.

Analog Screening Based on the Lead Compound MI-2

Similarity searching was set to a 0.7 cutoff and performed using the Collaborative Drug Discovery (CDD, Burlingame, CA) Database's (www.collaborativedrug.com) similarity search function. The CDD search function is based on ChemAxon's (www.chemaxon.com, Budapest, Hungary) standard Tanimoto similarity functions of hashed fingerprints as described in (<http://www.chemaxon.com/jchem/doc/dev/search/index.html#simil>). Briefly, hashed fingerprints of

every query structure are calculated and then the dissimilarity formula is applied as: $1 - (N_{A\&B} / (N_A + N_B - N_{A\&B}))$, Where N_A and N_B are the number of bits set in the fingerprint of molecule A and B, respectively, $N_{A\&B}$ is the numbers of bits that are set in both fingerprints. The dissimilarity threshold is a number between 0 and 1, which specifies a cutoff limit in the similarity calculation. If the dissimilarity value is less than the threshold, then the query structure and the given database structure are considered similar. Analogue screening was performed using the same methods as in primary screening, except it was done in triplicates. 19 compounds with higher activity than MI-2 were selected for further validation.

NMR

Uniformly ^{15}N and ^{13}C labeled MALT1 (329-728) was expressed in BL21 (DE3) *E. coli* growing in M9 medium containing 1g/l [^{15}N] ammonium chloride and 3g/l [^{13}C] glucose (Cambridge Isotope Labs, Andover, MA) and purified from *E. coli* cell lysate as described in (Wiesmann et al., 2012).

Standard 2D ^1H ^{13}C NMR spectra of MALT1 (329-728) were recorded in samples containing 10.0 mg/ml protein in 50 mM HEPES (pH 7.5), 50 mM NaCl, and 10 % D_2O . NMR spectroscopy experiments were recorded on Bruker AV 500 MHz spectrometer (Bruker, Billerica, MA), at 310K.

Standard 2D ^1H ^{15}N HSQC spectra of MALT1 (329-728) were recorded in samples containing 70 μM protein in 25 mM Tris pH 7.5, 250 mM NaCl, 5 mM DTT, 10% D_2O , 0.02% NaN_3 , 2% DMSO. HSQCs were run on a 600 MHz Varian (Varian, Palo Alto, CA) at 37 °C.

HPLC/ESI-MS

HPLC/ESI-MS experiments were carried out on 5 μl sample at 1 mg/ml protein concentration. Separation of proteins was performed on a HP1100 system (Hewlett Packard, Palo Alto, CA, USA) employing a 1 mm x 150 mm LC Packings column packed with POROS R1/H (Perseptive Biosystems, Foster City, CA, USA). The column was kept at 80 °C. Samples were injected onto the column using a CTC PAL autosampler (CTC, Zwingen Switzerland) fitted with a Valco model C6UW HPLC valve (Valco, Houston, TX, USA) and a 10 μl injection loop. HPLC was controlled by MassLynx

software (Micromass, Manchester, UK). UV detection was performed at 214 nm. Eluent A was water containing 0.05% TFA. Eluent B was a 1:9 mixture of water:acetonitrile containing 0.045% TFA. A gradient from 20% B to 90% B was run in 20 minutes. The flow rate was typically 60 μ l/min. The total flow from the LC system was introduced into the UV detection cell prior to introduction in the ESI source. The HPLC system was controlled and the signal from the UV detector was processed using MassLynx software. Mass spectroscopy was carried out using a Q-tof (Micromass, Manchester, UK) quadrupole time-of-flight hybrid tandem mass spectrometer equipped with a Micromass Z-type electrospray ionization source. Acquisition mass range was typically m/z 500-2000. Data were recorded and processed using MassLynx software. Calibration of the 500-2000 m/z scale was achieved by using the multiple-charged ion peaks of horse heart myoglobin (MW 16,951.5 Da).

Dose-Effect and Time-Course of MALT1 Inhibition

In a 384 well black plate (Greiner Bio One, Wemmel Belgium, catalogue # 784076), 8 pMole of purified LZ-MALT1 were incubated with compound MI-2 at different concentrations (125, 62.5, 31.25, 15.625, 7.8125 or 0 μ M) for indicated time (from 5 minutes to 80 minutes) at room temperature in buffer containing 5% DMSO, 20 mM HEPES pH 7.5, 10 mM KCl, 1.5 mM $MgCl_2$, 1 mM EDTA, 1 mM DTT, 0.01% TritonX-100, then 4 μ Mol of Ac-LRSR-AMC were then added into each mixture to initiate reactions. The reactions were monitored in a SpectraMax M5 plate reader (Molecular Devices, Sunnyvale, California USA) with excitation/emission wavelength at 360/465 nm and 20 seconds intervals. Normalized percentage of inhibition was calculated with the following formula: $(M_{(T_2-T_1)} - N_{(T_2-T_1)}) / (P_{(T_2-T_1)} - N_{(T_2-T_1)}) * 100$, where $M_{(T_2-T_1)}$ is the difference signal of compound at time point 200s and 0s, $N_{(T_2-T_1)}$ is the difference signal of negative control buffer only, $P_{(T_2-T_1)}$ is the difference signal of positive control Z-VRPR-FMK.

MI-2 Docking to MALT1

The structure of MI-2 was generated and its geometry was optimized. The atomic coordinates of MALT1 containing its paracaspase and Ig3 domains in complex with the Z-VRPR-FMK peptide

inhibitor (PDB ID: 3UOA) (Wiesmann et al., 2012; Yu et al., 2011) were chosen for inhibitor docking. After removing the peptide inhibitor and solvent molecules, hydrogen atoms were added to the MALT1 structure. The docking simulation started with defining 3D potential grids for MALT1 against MI-2. The calculated grid maps were of dimensions 60 × 40 × 40 points with the spacing of 0.375 Å/point. The generic algorithm in AutoDock 4.2 (Morris et al., 2009) was used and the docking was performed with MALT1 as a rigid molecule while allowing flexibility in the MI-2 inhibitor. The final results were ranked based on the predicted binding free energy.

Western Blot

Equal amounts of total protein (20-75 µg) were separated on sodium dodecyl sulfate–polyacrylamide gel electrophoresis (SDS-PAGE), and electrotransferred onto nitrocellulose membranes. Membranes were incubated with primary antibodies (MALT1, BCL-10, CYLD from Santa Cruz Biotechnologies, Santa Cruz, CA; A20 from eBioscience, San Diego, CA; phospho-IκB-α, IκB-α, c-REL, RELB from Cell Signaling, Danvers, MA and α-Tubulin from Sigma), followed by secondary antibodies conjugated to horseradish peroxidase, which were detected by chemiluminescence (Pierce, Thermo Scientific, Rockford, IL).

Flow Cytometry

To study the effect of MI-2 in cell proliferation, cells were labeled with carboxyfluorescein diacetate succinimidyl ester (CFSE, Invitrogen, Life Technologies, Grand Island, NY) at 0.5 µM and 37° C for 10 minutes. CFSE covalently labels long-lived intracellular molecules with carboxyfluorescein. Following each cell division, fluorescent molecules dilute in daughter cells, allowing comparative study of the kinetics of cell division. Cells were stained with DAPI (Sigma), followed by flow cytometry. DAPI^{neg} cells were gated for analysis.

To determine cell-cycle distribution, cells were analyzed by flow cytometry using pulse-BrdU (bromodeoxyuridine) incorporation with the APC BrdU Flow Kit (BD Pharmingen, San Jose, CA).

Apoptosis was assessed by AnnexinV-APC/DAPI (BD Pharmingen) staining followed by flow

cytometry.

Nuclear export of c-REL was studied by flow cytometry. Cells were treated as indicated and total cells or isolated nuclei were prepared and stained for c-REL. Total cells were fixed and permeabilized using the Intrastain kit from Dako (Glostrup, Denmark). For nuclei extraction, cells were resuspended in cold nuclei extraction buffer (320 mM sucrose, 5 mM MgCl₂, 10 mM HEPES, 1% Triton X-100 at pH 7.4), incubated for 10 min on ice and washed twice with nuclei wash buffer (320 mM sucrose, 5 mM MgCl₂, 10 mM HEPES at pH 7.4, no Triton X-100). Nuclei yield and integrity were confirmed by microscopic examination with trypan blue staining. For labeling, nuclei wash buffer was supplemented with 1% BSA, 0.1% sodium azide and 1:100 c-REL antibody (Cell Signaling). Cells were washed then incubated with Alexa Fluor-488 conjugated secondary antibodies from Invitrogen. Cells were washed again and stained with DAPI followed by flow cytometry.

Luciferase Assays

Reporter assays were performed in 293T cells seeded at a density of 2×10^5 cells per well of a 12-well dish. 100 ng of (NF- κ B)₅-Luc2CP-pGL4 and 10 ng of TK-Renilla internal control plasmid were cotransfected along with 25 ng of the indicated plasmids (MIGR1-MALT1^{WT} or MIGR1-MALT1^{C464A} and pcDNA4-Flag-Bcl10) using Lipofectamine 2000 (Invitrogen). Lysates were submitted to dual luciferase assays following manufacturer's protocol (Promega). In HBL-1, 5 μ g of (NF- κ B)₅-Luc2CP-pGL4 and 50 ng of TK-Renilla internal control plasmid per 5×10^6 cells were cotransfected using nucleofection (Amaxa, Lonza, Basel, Switzerland). Forty-eight hours after transfection, cells were plated at a density of 5×10^4 cells per well of a 24-well plate and treated as indicated. Lysates were submitted to dual luciferase assays following manufacturer's protocol (Promega).

Microarray Data Analysis

RNA from HBL-1 and TMD8 cells treated for 8 hours with compound MI-2 or vehicle at indicated concentrations and mRNA was isolated using the RNeasy Plus kit (Qiagen, Valencia, CA) followed by DNase treatment using the RNase-Free DNase reagent (Qiagen). RNA integrity was determined

using the RNA 6000 Nano LabChip Kit on an Agilent 2100 Bioanalyzer (Agilent Technologies, Santa Clara, CA). Samples were processed following Illumina recommendations and cRNA was hybridized to the HumanHT-12 v4 Expression BeadChip (Illumina, San Diego, CA). Arrays were scanned on the iScan system. Data pre-processing and quality control were performed using GenomeStudio. The data were \log_2 -transformed combined with quantile normalization (Du et al., 2008). GEO accession number GSE40003.

In order to determine the biological significance of the results, enrichment tests with respect to sets of related genes were carried out. To this end, we used GSEA (Gene Set Enrichment Analysis) software, and datasets were pre-ranked by fold change value (Subramanian et al., 2005). The p-values for each gene-set were computed on the basis of 1,000 iterations and multiple hypotheses testing correction for FDR calculation (Storey and Tibshirani, 2003).

Mouse Xenograft Experiments

Eight-week old male SCID NOD.CB17-Prkdc^{scid}/J mice were purchased from Jackson Laboratories (Bar Harbor, MN) and housed in a clean environment. Mice were subcutaneously injected with low-passage 10^7 human HBL-1, TMD8 or OCI-Ly1 cells in 50% matrigel (BD Biosciences, #354234). Treatment was initiated when tumors reached an average size of 120 mm³ (17 days post-transplantation). Drugs were reconstituted in DMSO and stored at -80° C until used and were administered by intra-peritoneal injection. Tumor volume was monitored by three-weekly digital calipering (Fisher Scientific, Thermo Scientific, Rockford, IL) and calculated using the formula (smallest diameter² × largest diameter)/2. Data were expressed as mean ± SEM, and differences were considered statistically significant at $p < 0.05$ by paired Student's t-test. All procedures involving animals followed US NIH protocols and were approved by the Animal Institute Committee of the Weill Cornell Medical College of Cornell University.

Immunofluorescence in Paraffin (IF-P) and Immunohistochemistry (IHC)

Paraffin-embedded tumor xenografts were sectioned, dewaxed and submitted to antigen retrieval. For

IF-P, Alexa Fluor-488 conjugated secondary antibodies from Invitrogen where used and cell nuclei where counterstained with DAPI. Fluorescent images were taken using an Axiovert 200M fluorescent microscope (Carl Zeiss Inc., Thornwood, NY).Oberkochen, Germany). For IHC, biotin-conjugated secondary antibodies where used. Then avidin/biotin peroxidase was applied to the slides (Vector Laboratories). Color was developed with diaminobenzoate chromogen peroxidase substrate (Vector) and counterstained with hematoxylin-eosyn. Pictures were obtained using an AxioCam (Carl Zeiss Inc.) camera attached to an AxioSkop II light microscope (Carl Zeiss Inc.). Samples were reviewed by a pathologist.

TUNEL

Terminal deoxynucleotidyl transferase dUTP nick end labeling, TUNEL assay (ApopTag, Chemicon, Temecula, CA), was used to detect apoptotic DNA fragmentation (Gavrieli et al., 1992). Briefly, formalin-fixed paraffin-embedded xenografted tumors were deparaffinized and pre-treated with trypsin (Zymed, San Francisco, CA) to expose DNA. Endogenous peroxidase was quenched using 3% hydrogen peroxide (Sigma) followed by incubation with TdT enzyme for 1 hour. Then, anti-digoxigenin-peroxidase was applied to the slides. Color was developed with diaminobenzoate chromogen peroxidase substrate (Vector Laboratories, Burlingame, CA) and counterstained with methyl green (Fisher Scientific, Thermo Scientific, Rockford, IL). Pictures were obtained using an AxioCam (Carl Zeiss Inc.) camera attached to an AxioSkop II light microscope (Carl Zeiss Inc.). Samples were reviewed by pathologist.

Supplemental References

Du, P., Kibbe, W. A., and Lin, S. M. (2008). lumi: a pipeline for processing Illumina microarray. *Bioinformatics* 24, 1547-1548.

Gavrieli, Y., Sherman, Y., and Ben-Sasson, S. A. (1992). Identification of programmed cell death in situ via specific labeling of nuclear DNA fragmentation. *J Cell Biol* 119, 493-501.

Lam, L. T., Davis, R. E., Pierce, J., Hepperle, M., Xu, Y., Hottelot, M., Nong, Y., Wen, D., Adams, J., Dang, L., and Staudt, L. M. (2005). Small molecule inhibitors of I κ B kinase are selectively toxic for subgroups of diffuse large B-cell lymphoma defined by gene expression profiling. *Clin Cancer Res* 11, 28-40.

Storey, J. D., and Tibshirani, R. (2003). Statistical significance for genomewide studies. *Proc Natl Acad Sci U S A* 100, 9440-9445.

Subramanian, A., Tamayo, P., Mootha, V. K., Mukherjee, S., Ebert, B. L., Gillette, M. A., Paulovich, A., Pomeroy, S. L., Golub, T. R., Lander, E. S., and Mesirov, J. P. (2005). Gene set enrichment analysis: a knowledge-based approach for interpreting genome-wide expression profiles. *Proc Natl Acad Sci U S A* 102, 15545-15550.